

Isoindolinone-based inhibitors of the MDM2–p53 protein–protein interaction

Ian R. Hardcastle,^{a,*} Shafiq U. Ahmed,^b Helen Atkins,^b A. Hilary Calvert,^b Nicola J. Curtin,^b Gillian Farnie,^b Bernard T. Golding,^a Roger J. Griffin,^a Sabrina Guyenne,^a Claire Hutton,^b Per Källblad,^c Stuart J. Kemp,^a Martin S. Kitching,^a David R. Newell,^b Stefano Norbedo,^a Julian S. Northen,^a Rebecca J. Reid,^a K. Saravanan,^a Henriëtte M. G. Willems^c and John Lunec^{b,*}

^aNorthern Institute for Cancer Research, School of Natural Sciences—Chemistry, Bedson Building, University of Newcastle upon Tyne, Newcastle upon Tyne, NE1 7RU, UK

^bNorthern Institute for Cancer Research, Paul O’Gorman Building, Medical School, Framlington Place, University of Newcastle upon Tyne, Newcastle upon Tyne, NE2 4HH, UK

^cDe Novo Pharmaceuticals, Compass House, Vision Park, Histon, Cambridge CB4 9ZR, UK

Received 22 November 2004; revised 17 December 2004; accepted 21 December 2004

Available online 30 January 2005

Abstract—A series of 2-*N*-alkyl-3-aryl-3-alkoxyisoindolinones has been synthesised and evaluated as inhibitors of the MDM2–p53 interaction. The most potent compound, 3-(4-chlorophenyl)-3-(4-hydroxy-3,5-dimethoxybenzyloxy)-2-propyl-2,3-dihydroisoindol-1-one (NU8231), exhibited an IC₅₀ of 5.3 ± 0.9 μM in an ELISA assay, and induced p53-dependent gene transcription in a dose-dependent manner, in the SJS human sarcoma cell line.

© 2005 Elsevier Ltd. All rights reserved.

The p53 tumour suppressor acts as a ‘guardian of the genome’ by reacting to cellular stress, such as hypoxia and DNA damage. Such stresses increase cellular levels of p53 and activate its transcriptional function to drive the expression of a number of genes that govern progression through the cell cycle, the initiation of DNA repair, and programmed cell death.^{1,2} The activity of p53 is tightly regulated by the MDM2 protein, the gene for which is itself regulated by p53. MDM2 binds to the p53 transactivation domain, blocking the transcriptional activity of p53 and ubiquitinating the MDM2–p53 complex to target it for proteosomal destruction. In normal cells the balance between active p53 and inactive MDM2-bound p53 is maintained by this negative feedback loop.^{3,4} The X-ray crystal structure of MDM2 bound to a p53 peptide corresponding to the transacti-

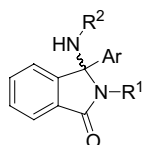
vation loop, reveals a hydrophobic pocket on the surface of MDM2, into which the Phe19, Trp23 and Leu26 residues of p53 bind.⁵ Inactivation of p53 through mutation is frequently found in a wide range of sporadic cancers. However, around 7% of human tumours show evidence of amplification and overexpression of the MDM2 gene resulting in suppression of functional p53, promoting transformation and uncontrolled tumour growth.⁶ Inhibitors of the MDM2–p53 binding interaction would be expected to restore normal p53 activity in MDM2 overexpressing cells and thus exert an anti-tumour effect.⁷ A number of inhibitors of the MDM2–p53 interaction have been reported including potent peptide inhibitors,⁸ the natural product chlorofusin,⁹ and small molecules including the recently described ‘nutlins’.^{10,11}

Here we describe inhibitors of the MDM2–p53 interaction, based on an isoindolinone scaffold. Preliminary screening studies, using an *in vitro* p53–MDM2 binding assay, identified compounds **1a** and **2a,b** as modest inhibitors of the p53–MDM2 interaction (IC₅₀

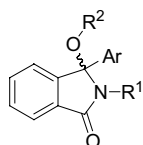
Keywords: Cancer; MDM2; p53; Protein–protein interactions.

* Corresponding authors. Tel.: +44 191 222 6645; fax: +44 191 222 8591 (I.R.H.); tel.: +44 191 246 4420 (J.L.); e-mail addresses: i.r.hardcastle@ncl.ac.uk; john.lunec@ncl.ac.uk

($\sim 200 \mu\text{M}$). These compounds also displayed growth inhibitory activity in the NCI 60 cell-line screen and, importantly, were COMPARE negative with respect to any known class of anti-tumour agents.¹² In this paper, we report a programme of focused library synthesis, incorporating in silico ligand design, resulting in the discovery of novel inhibitors of the MDM2–p53 interaction.



1a: $\text{R}^1 = \text{CH}_2\text{Ph}$; $\text{R}^2 = n\text{-Pr}$; $\text{Ar} = \text{Ph}$



2a: $\text{R}^1 = \text{CH}_2\text{Ph}$; $\text{R}^2 = n\text{-Pr}$; $\text{Ar} = \text{Ph}$
2b: $\text{R}^1 = \text{R}^2 = n\text{-Pr}$; $\text{Ar} = \text{Ph}$

Using the published structure of the MDM2–p53 binding site,⁵ we have employed computational methods, and focussed library synthesis based on the isindolinone template, to develop compounds with improved inhibitory activity. These studies have resulted in the identification of a number of inhibitors (Table 1) with increased potency over the preliminary compounds (**1a** and **2a,b**).

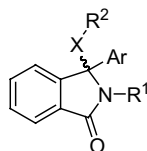
Briefly, the determination of single, low-energy binding modes for **1a** and **2b** was attempted by docking the compounds into the published crystal structure of MDM2

(1YCR)⁵ using easyDock.¹³ A single plausible binding mode was chosen for each compound, and the position of the isindolinone scaffold was preserved during the following virtual screen of new substituents. The binding interaction between ligand and receptor was explored using a simulated annealing optimisation of an empirical free-energy function using the program Skelgen.¹⁴ Reagents able to form at least one additional H-bond with target residues of MDM2 were selected as ‘virtual hits’ and suggested for synthesis, a selection of which were synthesised. Comparison of the inhibitory activity of these synthesised ‘virtual hits’ with a set of isindolinones bearing randomly selected substituents revealed no significant difference in activity between the two sets (data not shown).

At this point, the binding mode determination was revisited with the six most active compounds synthesised (Table 1). The six lead compounds were docked into the MDM2 crystal structure 1YCR, using the programs easyDock¹³ and GOLD.¹⁵ It was impossible to distinguish a single preferred binding mode from the large pool of docking solutions. Previously, it has been shown that the probability of predicting the experimental binding mode correctly increases significantly when multiple binding modes are considered.¹⁶ Therefore, a total of 24 (6 per compound \times 2 per stereoisomer \times 2 per docking program) high scoring, unique binding modes were selected as starting points for a second round of virtual screening. Again, reagents able to form additional hydrogen bonds with the protein were suggested for synthesis.

Table 1. Seed compounds used in the second round of binding mode determinations

X	Ar	R ¹	R ²	IC ₅₀ (μM)
NH		<i>n</i> -Pr		27 \pm 3
NH		<i>n</i> -Pr		66 \pm 8
O	Ph		<i>n</i> -Pr	90 \pm 39
NH	Ph			85
O	Ph			92 \pm 11
NH	Ph			70 \pm 8



In order to validate this approach 57 hit compounds were selected, including substituents unique to each binding mode. The majority of these compounds were synthesised and assayed for inhibition of MDM2–p53 binding using the ELISA format assay. A number of compounds that displayed improved activity were identified including **2e,f** and **2g** (Table 2).

Consideration of these results and others from additional isoindolinones synthesised as part of random libraries, enabled the design of a combinatorial array of compounds bearing the N-2 and C-3 substituents that appeared to confer improved activity. The substituents chosen were: Ar = phenyl, 4-(2-trimethylsilylethoxy)-methoxyphenyl and 4-chlorophenyl; R¹ = *n*-propyl, benzyl and 2-acetamidoethyl; R² = 4-*t*-butylbenzyloxy, 3,5-dimethoxy-4-hydroxybenzyloxy, 2-(2-pyridyl)ethoxy and 3-hydroxypropoxy.

Compounds **2a–z** were prepared according to Methods A, B and C (Scheme 1). The appropriate benzoylbenzoic acids (**3**) were converted into the ψ -acid chlorides (**4**), under Vilsmeier conditions, and then condensed with the R¹-primary amine to give the 4-hydroxyisoindolinone (**5**). Compound **5** was converted into the chloride and subsequently reacted with R²-alcohol in the presence of base (Et₃N or K₂CO₃) to give **2d,e,g–m,o–r** and **2u,v** (Method A).¹⁷ Alternatively, compound **5** was converted into the unstable chloride and trapped with benzylmercaptan to give the stable thioether (**6**). This was activated to nucleophilic displacement on treatment with N-iodosuccinimide (NIS) in the presence of catalytic camphorsulfonic acid (CSA) and reacted in situ with the appropriate R²-alcohol to give **2a,f,n,s** and **t**. Compounds **2w–z** were prepared according to Method C (Scheme 1). Directed-*ortho*-metallation of *n*-propylbenzamide (**7** R¹ = *n*Pr) and reaction with the appropriate benzoate ester afforded the hydroxyisoindolinone **5**, which was converted into the target isoindolinone as for Method A. The final compounds **2h–z** were isolated and tested as racemic mixtures.¹⁸

Compounds were assayed for inhibition of the MDM2–p53 interaction using a 96-well plate binding assay (ELISA) with a luminometric detection end-point. Briefly, 96-well plates were coated with streptavidin followed by biotinylated IP3 peptide (b-IP3: Biotin-Met-Pro-Arg-Phe[19]-Met-Asp-Tyr-Trp-Glu-Gly-Leu[26]-Asn-NH₂).¹⁹ Control experiments consisted of both 5% DMSO carrier alone as a negative control and 100 nM active peptide (AP-B: Ac-Phe[19]-Met-Aib-Pmp-6-Cl-Trp-Glu-Ac₃-Leu[26]-NH₂) as a positive control peptide antagonist of the MDM2–p53 interaction (IC₅₀ = 5 nM).⁸ Compounds and controls were pre-incubated at 20 °C for 20 min with MDM2, before transfer of the MDM2-compound mixture to the b-IP3 streptavidin plates and incubation at 4 °C for 90 min. After washing to remove unbound MDM2, each well was incubated at 20 °C with a buffered solution of primary anti-MDM2 antibody (Ab-5, Calbiochem), then washed and incubated at 20 °C with a solution of secondary horseradish peroxidase (HRP) conjugated antibody (Dako), and washed again. The HRP activity was measured by

enhanced chemiluminescence (ECLTM, Amersham Biosciences) using the oxidation of the diacylhydrazide substrate, luminol, to generate a quantifiable light signal. The luminol substrate together with enhancer was automatically injected into each well and the relative luminescence units (RLU) measured over a 30 s interval using a Berthold MicroLumat-Plus LB 96V microplate luminometer. The percentage MDM2 inhibition at a given concentration was calculated as the (RLU detected in the compound treated sample ÷ RLU of DMSO controls) × 100. The IC₅₀ was calculated using a plot of %MDM2 inhibition versus concentration and is the average of three independent experiments. The results are presented in Table 2.

In comparison with the lead compounds bearing an unsubstituted phenyl group at the C3 position (**2d,e** and **g**), none of the newly synthesised compounds displayed improved potency, with only the syringic alcohol derivative **2k** and the 2-(2-pyridyl)ethoxy derivative **2m** showing inhibition comparable with the 4-*t*-butylbenzyloxy derivative **2d**. In the 3-(4-chlorophenyl) series, the *N*-propyl substituted 3-hydroxypropoxy derivative **2r** was equipotent with the lead *N*-benzyl compound **2c**. In contrast, the *N*-propyl substituted 2-(2-pyridyl)ethoxy derivative **2s** was significantly less potent than the lead *N*-benzyl compound **2f**. The reverse trend was observed for the *N*-propyl syringic alcohol derivative **2q**, which was significantly more potent than the *N*-propyl derivative **2o**. Interestingly, for the syringic alcohol derivatives, the 4-chloro substituent was favourable in the *N*-propyl series (**2k** and **2q**) but resulted in a loss of potency in the *N*-benzyl series (**2i** and **2j**). In the *N*-ethylacetamido series, the 3-(4-chlorophenyl) derivatives (**2v** and **2w**) were significantly less potent than the lead **2g**. In the light of these disappointing results, and the difficulties encountered with the synthesis of these derivatives, this series was abandoned. Similarly, in the 4-(2-trimethylsilylethoxy)methoxyphenyl series, none of the compounds synthesised (**2v–z**) displayed improved potency compared with the lead **1b** and the series was not completed.

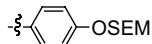
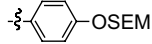
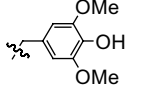
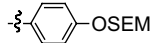
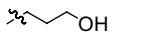
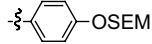
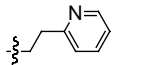
The increased potency observed for the 4-chlorophenyl compound **2q**, is consistent with the predicted binding mode for the parent **2g**, which is seen bound to MDM2 with the phenyl ring occupying the tryptophan binding pocket, the *N*-propylisoindolinone in contact with a broad, shallow, hydrophobic cleft and the phenolic OH of the syringic alcohol making an H-bond to the backbone of Tyr100 on MDM2 (Fig. 1). The importance of the tryptophan binding pocket for affinity has been demonstrated previously by the potent activity of the AP peptide,⁸ and the nutlin series.^{10,20} Experiments to confirm the binding mode of **2q** are ongoing.

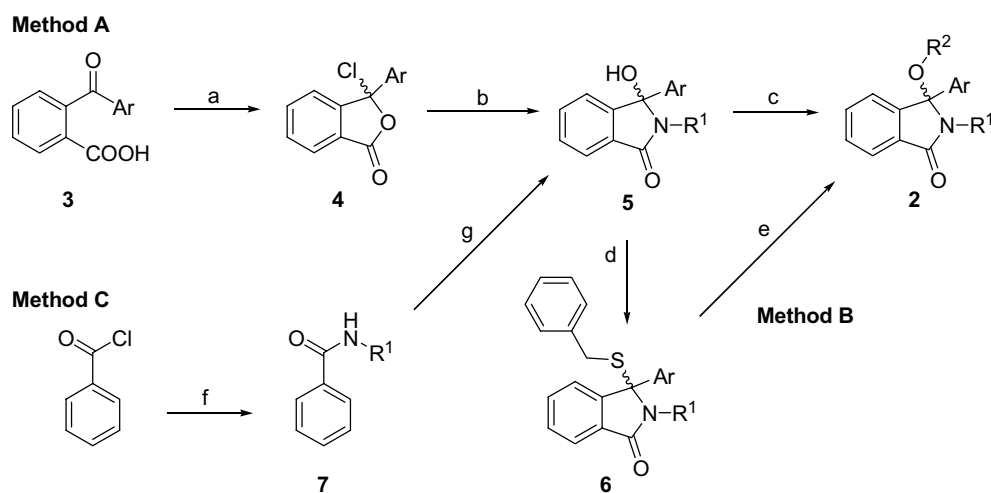
The most potent compound identified, **2q** (NU8231; IC₅₀ = 5.3 ± 0.9 μM), was selected for further evaluation. SJSA cells, in which the MDM2 gene is amplified, were treated with increasing concentrations (5, 10 and 20 μM) of **2q**. Cells were lysed at 6 h and protein extracts analysed by Western immunoblotting for p53, p21^{WAF1} and actin (Fig. 2). There was a dose-dependent

Table 2. Inhibition of the MDM2–p53 binding interaction by isoindolinones

Compound	Method	Ar	R ¹	R ²	IC ₅₀ (μM)
2c	B				15.9 ± 0.8
2d	A	Ph			92 ± 11
2e	A	Ph			14 ± 0.3
2f	B				26.2 ± 4.2
2g	A	Ph			17.9 ± 0.3
2h	A	Ph			245
2i	A	Ph			206 ± 30
2j	A	Ph	<i>n</i> -Pr		>500
2k	A	Ph	<i>n</i> -Pr		82 ± 8
2l	A	Ph	<i>n</i> -Pr		>500
2m	A	Ph	<i>n</i> -Pr		100 ± 14
2n	B				99 ± 18
2o	A				42 ± 8
2p	A		<i>n</i> -Pr		187 ± 38
2q	A		<i>n</i> -Pr		5.3 ± 0.9
2r	A		<i>n</i> -Pr		16.4 ± 1.6
2s	B		<i>n</i> -Pr		57 ± 6
2t	B				91.4 ± 0.4
2u	A				76 ± 4
2v	A				257 ± 34

Table 2 (continued)

Compound	Method	Ar	R ¹	R ²	IC ₅₀ (μM)
2w	C		<i>n</i> -Pr		464 ± 31
2x	C		<i>n</i> -Pr		118 ± 24
2y	C		<i>n</i> -Pr		476 ± 24
2z	C		<i>n</i> -Pr		312 ± 22



Scheme 1. Reagents and conditions: Method A: (a) SOCl₂, cat DMF, THF; (b) R¹NH₂, THF; (c) (i) SOCl₂, cat DMF, THF; (ii) R²OH, THF, Et₃N or K₂CO₃. Method B: (d) (i) SOCl₂, cat DMF, THF; (ii) PhCH₂SH, THF; (e) NIS, cat CSA, THF, R²OH. Method C: (f) R¹-NH₂, (g) *s*-BuLi, ArCOOEt, THF.

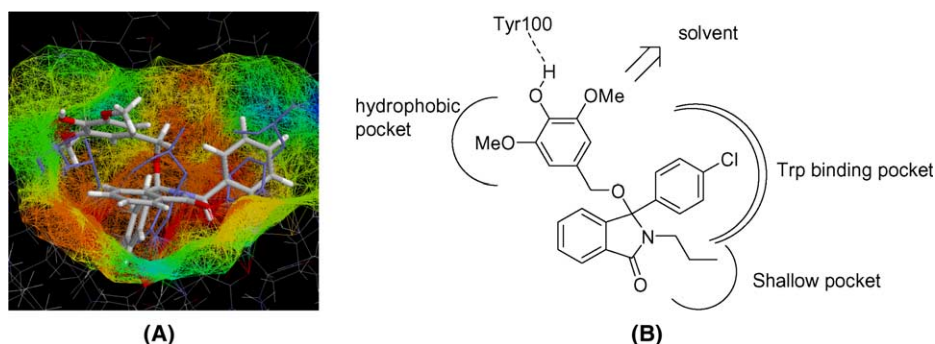


Figure 1. A—Model of the low energy binding mode of **2g** bound to MDM2. B—Pharmacophore model of **2q** bound to MDM2.

increase in MDM2 and p21, consistent with p53 activation. No change was observed for p53 levels or the actin controls.

In summary, we have discovered interesting structurally-novel isoindolinone antagonists of the MDM2–p53 pro-

tein–protein binding interaction. The most potent compound **2q** has an IC₅₀ of 5.3 ± 0.9 μM in a cell-free binding assay (ELISA) and shows dose-dependent induction of MDM2 and p21 when used to treat an intact MDM2 amplified human sarcoma cell line. Further development of these compounds is in progress.

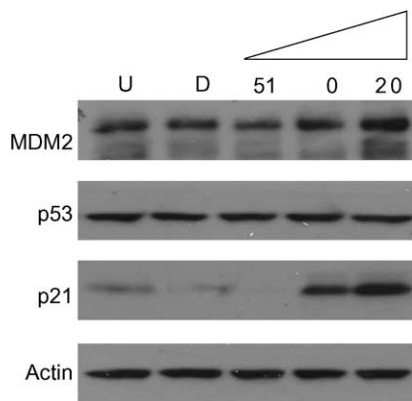


Figure 2. Western blot from SJSa cells treated with **2q** (U: untreated; D: DMSO control; 5, 10 and 20 μ M compound **2q**).

Acknowledgements

The authors thank Cancer Research UK, EPSRC and BBSRC for financial support. The authors are grateful to Dr Edward Sausville and Dr. Robert Schultz of the DTP, National Cancer Institute, Washington, USA, for facilitating the analysis of compounds in the NCI cell line panel.

References and notes

- Lane, D. P. *Nature* **1992**, *358*, 15–16.
- Vousden, K. H.; Lu, X. *Nat. Rev. Cancer* **2002**, *2*, 594–604.
- Momand, J.; Zambetti, G. P.; Olson, D. C.; George, D.; Levine, A. *Cell* **1992**, *69*, 1237–1245.
- Fuchs, S. Y.; Adler, V.; Buschmann, T.; Wu, X. W.; Ronai, Z. *Oncogene* **1998**, *17*, 2543–2547.
- Kussie, P. H.; Gorina, S.; Marechal, V.; Elenbaas, B.; Moreau, J.; Levine, A. J.; Pavletich, N. P. *Science* **1996**, *274*, 948–953.
- Oliner, J. D.; Kinzler, K. W.; Meltzer, P. S.; George, D. L.; Vogelstein, B. *Nature* **1992**, *358*, 80–83.
- Chene, P. *Nat. Rev. Cancer* **2003**, *3*, 102–109.
- Garcia-Echeverria, C.; Chene, P.; Blommers, M. J. J.; Furet, P. *J. Med. Chem.* **2000**, *43*, 3205–3208.
- Duncan, S. J.; Gruschow, S.; Williams, D. H.; McNicolas, C.; Purewal, R.; Hajek, M.; Gerlitz, M.; Martin, S.; Wrigley, S. K.; Moore, M. *J. Am. Chem. Soc.* **2001**, *123*, 554–560.
- Vassilev, L. T.; Vu, B. T.; Graves, B.; Carvajal, D.; Podlaski, F.; Filipovic, Z.; Kong, N.; Kammlott, U.; Lukacs, C.; Klein, C.; Fotouhi, N.; Liu, E. A. *Science* **2004**, *303*, 844–848.
- Zhao, J. H.; Wang, M. J.; Chen, J.; Luo, A. P.; Wang, X. Q.; Wu, M.; Yin, D. L.; Liu, Z. H. *Cancer Lett.* **2002**, *183*, 69–77.
- Paull, K. D.; Shoemaker, R. H.; Hodes, L.; Monks, A.; Scudiero, D. A.; Rubinstein, L.; Plowman, J.; Boyd, M. R. *J.N.C.I.* **1989**, *81*, 1088–1092.
- Mancera, R. L.; Källblad, P.; Todorov, N. P. *J. Comput. Chem.* **2004**, *25*, 858–864.
- Stahl, M.; Todorov, N. P.; James, T.; Mauser, H.; Boehm, H. J.; Dean, P. M. *J. Comput. Aided Mol. Des.* **2002**, *16*, 459–478.
- Jones, G.; Willett, P.; Glen, R. C.; Leach, A. R.; Taylor, R. *J. Mol. Biol.* **1997**, *267*, 727–748.
- Källblad, P.; Mancera, R. L.; Todorov, N. P. *J. Med. Chem.* **2004**, *47*, 3334–3337.
- Kitching, M. S.; Clegg, W.; Elsegood, M. R. J.; Griffin, R. J.; Golding, B. T. *Synlett* **1999**, 997–999.
- All compounds gave satisfactory ^1H and ^{13}C NMR, IR, LCMS and HRMS or combustion analysis.
- Bottger, V.; Bottger, A.; Howard, S. F.; Picksley, S. M.; Chene, P.; Garcia-Echeverria, C.; Hochkeppel, H. K.; Lane, D. P. *Oncogene* **1996**, *13*, 2141–2147.
- Fry, D. C.; Emerson, S. D.; Palmeb, S.; Vua, B. T.; Liua, C.-M.; Podlaskia, F. *J. Biomol. NMR* **2004**, *30*, 163–173.